RSC Advances

COMMUNICATION

View Article Online
View Journal | View Issue

Cite this: *RSC Adv.*, 2015, **5**, 59106

Received 21st May 2015
Accepted 19th June 2015

DOI: 10.1039/c5ra09570k

www.rsc.org/advances

A coordination and ligand replacement based three-input colorimetric logic gate sensing platform for melamine, mercury ions, and cysteine†

Lulu Zhang,[a] Yanwen Yuan,[a] Xinglin Wen,[a] Yue Li,[b] Cuong Cao*[c] and Qihua Xiong*[ad]

Discrimination of different species in various target scopes within a single sensing platform can provide many advantages such as simplicity, rapidness, and cost effectiveness. Here we design a three-input colorimetric logic gate, based on the aggregation and anti-aggregation of gold nanoparticles (Au NPs), for the sensing of melamine, cysteine, and Hg^{2+}. The concept makes use of the advantages of the highly specific coordination and ligand replacement reactions between melamine, cysteine, Hg^{2+}, and Au NPs. Different outputs are obtained with the combinational inputs in the logic gates, which can serve as a reference to discriminate different analytes within a single sensing platform. Furthermore, besides the intrinsic sensitivity and selectivity of Au NPs to melamine-like compounds, the "INH" gates of melamine/cysteine and melamine/Hg^{2+} in this logic system can be employed for sensitive and selective detections of cysteine and Hg^{2+}, respectively.

Introduction

Maintaining a healthy lifestyle has been one of the most pressing topics of concern around the world for decades, especially with the increasing issues of food safety, environmental contamination, and personal healthcare. In particular, the shocking scandals of melamine in infant formula in 2008, and in yoghurt candy in 2014 have further warned the general public that food safety is a long-lasting battle for the human society.[1,2] Heavy metal contaminants, such as mercury, on the other hand, represent one of the most severe environmental challenges.[3] As a sulphur-containing amino acid, cysteine plays a crucial biological role in the human body. It is also a potential neurotoxin at elevated levels,[4,5] a biomarker for various medical conditions,[6,7] and a disease-associated physiological regulator.[8–10] Therefore, a rapid and low-cost method for identification and detection of these targets is of crucial importance for environmental protection, food safety and medical diagnostics as well as for fundamental research. However, conventional methods employed in the sensing of Hg^{2+} (*e.g.* cold-vapor atomic fluorescence spectrometry,[11] cold-vapor atomic absorption spectrometry,[12] inductively coupled plasma-mass spectrometry,[13] and X-ray absorption spectroscopy[14]), melamine (*e.g.* high-performance liquid chromatography,[15] and mass spectroscopy[16]), and cysteine (*e.g.* electrochemical voltammetry,[17,18] and fluorescence-coupled HPLC techniques[19,20]) are often expensive, labour-intensive, time-consuming, and non-portable. Therefore, low cost, simple, rapid, and portable methods are highly desired.

In this context, colorimetric sensing based on analyte induced aggregation or anti-aggregation of Au NPs has been widely used in chemo/biosensors for the detection of various analytes owing to its integration of simplicity, rapidness and cost effectiveness.[21–27] In addition, the aggregation or anti-aggregation processes of Au NPs are often accompanied by a shift of the surface plasmon band, as well as a clear colour change between blue and red due to the inter-particle plasmon coupling,[28,29] which can be easily observed either by naked eye or simple spectroscopy measurements. However, every sensing method has its own strengths and weaknesses due to its own limitations. Until now, most of the colorimetric platforms based on Au NPs are designed to detect one certain target and cannot be employed for the discrimination of different species in various target scopes within a single sensing platform.

Molecular logic gates which use the concept of a logic gate to construct chemo/biosensors, provide a possible way of solving the above problem. Depending on the number and the relationship of the inputs in the system, a wide range of logic

[a]*Division of Physics and Applied Physics, School of Physical and Mathematical Sciences, Nanyang Technological University, Singapore 637371. E-mail: Qihua@ntu.edu.sg*

[b]*Key Laboratory of Materials Physics, Institute of Solid State Physics, Chinese Academy of Sciences, Hefei, 230031, P. R. China*

[c]*Institute for Global Food Security, School of Biological Sciences, Queen's University Belfast, 18-30 Malone Road, Belfast, BT9 5BN, UK. E-mail: c.cao@qub.ac.uk*

[d]*NOVITAS, Nanoelectronics Center of Excellence, School of Electrical and Electronic Engineering, Nanyang Technological University, Singapore 639798*

† Electronic supplementary information (ESI) available. See DOI: 10.1039/c5ra09570k

functions which include YES, NOT, AND, OR, NOR, NAND, INH, and XOR could be obtained.[30] Analytes can be distinguished through different signal outputs upon changing the inputs. Therefore, different types of molecular sensors based on logic gate operations have been developed for the sensing of various targets such as metal ions,[31,32] neurotransmitter release,[33] DNA and aptamer,[34] and iodide.[35] To date, colorimetric logic gates based on the aggregation or anti-aggregation of Au NPs are mostly formulated by two inputs due to the lack of highly specific interactions between multiple target species,[24,36–40] which thereby hampers the construction of a logically inter-connected sensing system with more than two inputs. Furthermore, the input species lack highly specific interactions with each other or Au NPs which may also lead to uncontrollable behaviour of the Au NPs. Therefore, ensuring highly specific interactions between the introduced species which serve as inputs, plays a key role in rationally designing a logic gate system with more inputs. Herein, we report a new three-input molecular logic gate for the sensing of melamine, cysteine, and Hg^{2+} based on the mechanism of analyte-induced aggregation and anti-aggregation of Au NPs. The aggregation and anti-aggregation of Au NPs can be well controlled due to the highly specific coordination and ligand replacement reactions between melamine, cysteine, Hg^{2+}, and Au NPs. Therefore, a variety of inter-connected logic gates with different logic operations which include AND, OR, and INH can be built depending on the type of interactions between the targeted species and Au NPs. The highly specific interactions between the targeted species and Au NPs endow the as-designed system with high selectivity to the targets. Furthermore, the intrinsic sensitivity of Au NPs to melamine, which has been carefully studied before,[23,41] enables the inter-connected sensing system to have good sensitivity to cysteine, and Hg^{2+}.

Experimental section

Materials and measurements

$Hg(ClO_4)_2 \cdot H_2O$, $CrCl_3 \cdot 6H_2O$, KCl, cyromazine, cyanuric acid, dicyandiamide, butylamine, acetonitrile, glycine, alanine, serine, proline, aspartic acid, asparagine, glutamic acid, ornithine, glutamine, histidine, tyrosine and arginine were of analytical grade and obtained from Sigma-Aldrich, Singapore. Cysteine, melamine, sodium citrate anhydrous, $HAuCl_4 \cdot 3H_2O$, $ZnCl_2$, $PbCl_2$, $CuCl_2 \cdot 2H_2O$, $CdCl_2$, $FeCl_3$, and $NiCl_2$ were purchased from Alfa Aesar. Ultrapure water (18 MΩ) was used for all solution preparations. UV-vis absorption spectra were acquired using a PerkinElmer LAMBDA 950 spectrophotometer. TEM was performed on a JEOL1400 transmission electron microscope with an accelerating voltage of 100 kV. The SEM image was acquired by scanning electron microscopy (SEM; JEOL JSM-7001F).

Synthesis of ~13 nm and ~30 nm Au NPs

~13 nm colloidal Au NPs were prepared by the reduction of $HAuCl_4$ with trisodium citrate in aqueous solution.[23] Typically, 10 mL of trisodium citrate (38.8 mM) was rapidly injected into a boiling solution of $HAuCl_4$ (100 mL, 1 mM), and the mixed solution was further refluxed for another 15 min into a wine red suspension. The suspension was gradually cooled to room temperature under stirring. The concentration of the Au NPs as determined by UV-vis spectroscopy was 10 nM. Then 10 mL of the Au NP suspension was diluted with 50 mL of deionised water to give a total volume of 60 mL as a stock liquid for the sensing of analytes. ~30 nm colloidal Au NPs were prepared by a similar method. Typically, 0.25 mL of 0.1 M $HAuCl_4$ was added to 100 mL of ultrapure water and then heated to boiling under magnetic stirring. After quickly injecting 1.5 mL of 1% trisodium citrate, the mixed solution was refluxed for 30 min and the Au NPs were synthesized. Then 10 mL of the Au NP solution was diluted with 10 mL of deionised water to give a total volume of 20 mL as a stock liquid for the sensing of analytes.

Operations of the colorimetric logic gates

For the logic gate operations, different analytes were mixed thoroughly first, and then added into 1 mL of the above ~13 nm Au NP suspension with the final effective concentration of the analytes at 6×10^{-5} M (melamine), 3.6×10^{-4} M (cysteine), and 1.8×10^{-4} M (Hg^{2+}). To eliminate the effect of dilution, the volume of the mixture of the analytes was less than 30 μL. After 2 minutes, absorbance spectra of Au NP solutions were recorded with a UV-vis spectrometer. Photos of the above Au NP solutions were also taken by a digital camera at the same time.

Sensing of melamine

For analysis, 10 μL of the melamine aqueous solution with certain concentration was added into 1 mL of the Au NP solution to study the aggregation degree of Au NPs. For selectivity experiments, 10 μL of one of the different nitrogen containing compounds in aqueous solution was added into 1 mL of the Au NP solution, the final effective concentrations of different nitrogen containing compounds in Au NP solutions were all 1.5×10^{-6} M. After mixing thoroughly for 2 minutes, absorbance spectra and photos of the Au NP solutions were recorded with a UV-vis spectrometer and digital camera.

Sensing of cysteine

For selectivity experiments, 10 μL of one of the different amino acids and 10 μL of melamine in aqueous solution were mixed thoroughly first, and then added into 1 mL of the Au NP solution, the final effective concentrations of the different amino acids and melamine were all 6×10^{-5} M. After mixing thoroughly for 2 minutes, the absorbance spectra and photos of the Au NP solutions were recorded with a UV-vis spectrometer and digital camera. To study the limit of detection of cysteine, 1 mL of Au NP solution with a degree of aggregation induced by melamine at a final concentration of 1.4×10^{-6} M was used as a control sample. 10 μL aliquots of cysteine at different concentrations and 10 μL of melamine in aqueous solution were mixed thoroughly, and then added to 1 mL of the Au NP solution. The final effective concentration of cysteine ranged from 0 to 3×10^{-6} M, whereas the final concentration of melamine was always 1.4×10^{-6} M. After mixing thoroughly for 2 minutes, the

absorbance spectra and photos of the Au NP solutions were recorded with a UV-vis spectrometer and digital camera.

Sensing of Hg^{2+}

For selectivity experiments, 10 μL of one of the different metal ions and 10 μL of melamine in aqueous solution were mixed thoroughly first, and then added into 1 mL of the Au NP solution, the final effective concentrations of the different metal ions were all 5×10^{-6} M, whereas the final concentration of melamine was always 1.5×10^{-6} M. After mixing thoroughly for 2 minutes, the absorbance spectra and photos of the Au NP solutions were recorded with a UV-vis spectrometer and digital camera. To study the limit of detection of Hg^{2+}, the aggregation degree of 1 mL of Au NP solution induced by melamine at a final concentration of 6×10^{-7} M was used as a control sample in the presence of 15 mM NaCl. Then 10 μL of Hg^{2+} at different concentrations and 10 μL of melamine in aqueous solution were mixed thoroughly, and then added to 1 mL of the Au NP solutions, the final effective concentrations of Hg^{2+} ranged from 0 to 400 nM, whereas the final concentrations of melamine were all 6×10^{-7} M. After mixing thoroughly for 15 minutes, absorbance spectra and photos of Au NP solutions were recorded with a UV-vis spectrometer and digital camera.

Results and discussion

Design of the three-input Au NP colorimetric logic gate of Hg^{2+}, melamine, and cysteine

Fig. 1 illustrates the mechanism of the colorimetric logic gate. We define the inputs "1" and "0" of the logic gate as the presence and absence of an analyte, respectively. Then we can define the wine red (dispersed) and dark blue (aggregated) colour of Au NP aqueous solution as "0"and "1" which correspond to the outputs of a logic gate, respectively. Since there are three kinds of analytes (Hg^{2+}, melamine, and cysteine) in our system, the possible number of input conditions is $2^3 = 8$, namely, 000, 100, 001, 101, 111, 110, 011, and 010. The 13 nm colloidal Au NPs are wine red and well dispersed in aqueous solution with the weakly surface-bound, negatively charged citrate ions (input 000, output 0), whereas their aggregates appear dark blue in colour. Because melamine is positively charged owing to its protonated amine groups, addition of melamine to the Au NP solution will shield the electrostatic repulsion of negative charges that helps stabilize the Au NPs. As a result, the surface-bound citrate ions are depleted, subsequently leading to the cross linking of Au NPs or the aggregation of Au NPs accompanied by a colour change from wine red to dark blue (input 001, output 1). However, the aggregation of Au NPs induced by the addition of melamine can be easily inhibited in the presence of Hg^{2+} due to the higher affinity of melamine to Hg^{2+}, which can be explained by the coordination that occurs through the amine and triazine nitrogen atoms in melamine with Hg^{2+} (input 101, output 0).[42] Among various kinds of organic groups, the sulfhydryl group has superior affinity to the surface of Au NPs due to the formation of an Au–S bond which is commonly employed in the surface modification of Au NPs.[21,43] As a sulfhydryl-containing amino acid, cysteine could be chemisorbed onto the surface of Au NPs to form a molecular layer of cysteine (input 010, output 0). It is anticipated that the chemisorption of cysteine onto a Au surface is superior to the electrostatic coordination of melamine, therefore an addition of cysteine could prevent melamine from inducing the aggregation of Au NPs (input 011, output 0). On the other hand, since the breakage of Au–S bonds will occur when there is Hg^{2+} in the system, the addition of Hg^{2+} to the Au NPs solution in the presence of cysteine will lead to the removal of the chemisorbed thiolates on the Au surface.[26] This process destabilizes the well-dispersed Au NP solution, resulting in the aggregation of Au NPs (input 110, output 1). However, the addition of Hg^{2+} to the Au NP colloidal solution in the absence of cysteine has almost no effect on the dispersion state of Au NPs (input 100, output 0). Furthermore, in the presence of all inputs (Hg^{2+}, melamine, and cysteine), Hg^{2+} would rather bind to cysteine than melamine; this competition leads to the formation of a more stable Hg^{2+}–cysteine complex instead of a Hg^{2+}–melamine complex and subsequently results in the aggregation of Au NPs (input 111, output 1). Based on the coordination and ligand replacement mechanisms between Hg^{2+}, melamine, cysteine and Au NPs, the three-input colorimetric logic gate was rationally designed.

Combinational operations of the Au NP colorimetric logic gate

The synthesized Au NPs were characterized by TEM which indicates that their size is ~13 nm (Fig. S1, ESI†). Fig. 2A shows the responses of the absorption spectra of the 13 nm Au NP solutions upon the combinational additions of melamine, cysteine, and Hg^{2+}. Dramatic changes in the absorption spectra of the Au NPs are observed from samples upon the additions of melamine (input 001), melamine/Hg^{2+}/cysteine (input 111), and Hg^{2+}/cysteine (input 110). Absorption bands of the Au NPs in the range of 600 to ~700 nm resulted from their aggregates increasing obviously, while the original absorbance of the Au NPs at 520 nm decreases strongly. It is found that there are insignificant changes in the absorption spectra of the Au NPs upon the additions of melamine, cysteine, and Hg^{2+} in the other combinations which correspond to the input conditions 000, 100, 101, 011, and 010. The TEM images of the Au NPs upon the combinational additions of melamine, cysteine, and Hg^{2+} for the logic operations confirm their corresponding dispersion or aggregation states (Fig. S1, ESI†). It is consistent with the absorption spectra that the aggregates were only formed with the input conditions 001, 110, and 111. Furthermore, the corresponding colorimetric effects are evaluated by comparing the $A_{650\ nm}/A_{520\ nm}$ values (Fig. 2B). Fig. 2C depicts the network map of the combinations of the "AND", "INH", and "OR" gates for the logic operations. Neither Hg^{2+} nor cysteine can induce the aggregation of Au NPs alone, however, their coexistence would result in a dramatic aggregation of Au NPs. Thus, an "AND" gate could be built to convey the interrelationship between the presence of cysteine/Hg^{2+} and the aggregation of Au NPs. Since melamine alone also possesses the ability to enable Au NP aggregation, an "OR" gate can be employed to describe the logic connection between melamine and the "AND" gate of cysteine/

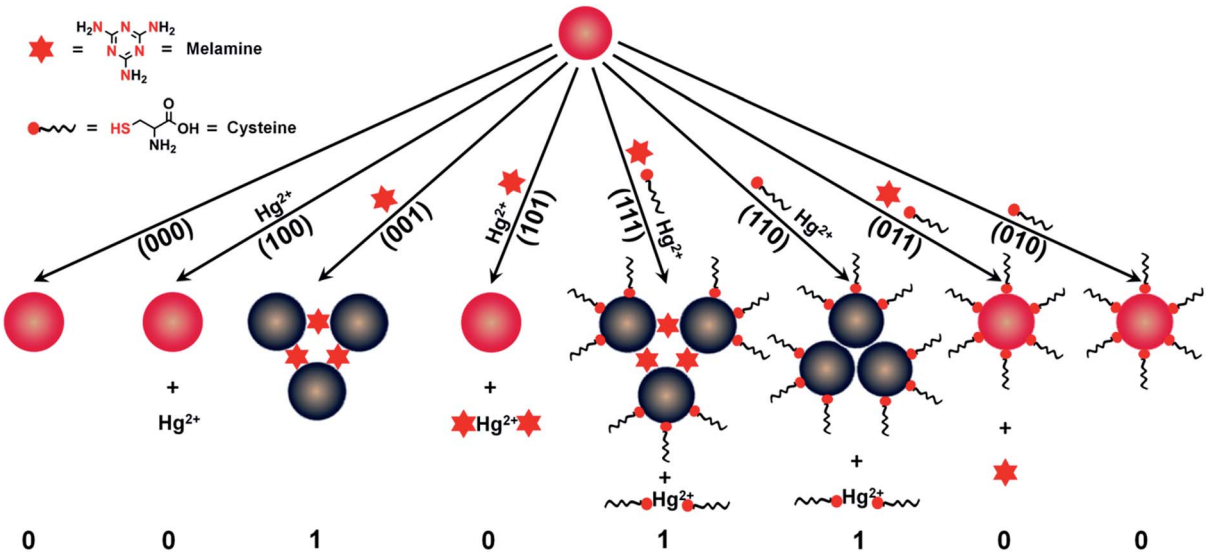

Fig. 1 A schematic illustration of the mechanism of the colorimetric logic gate.

Hg^{2+}. Meanwhile, the presence of only cysteine or Hg^{2+} can inhibit the aggregation of Au NPs induced by melamine. Therefore, two "INH" gates of melamine/cysteine and melamine/Hg^{2+} are also needed. The detailed logic operations of "AND", "OR", and "INH" gates are illustrated in Table S1 (ESI†). Fig. 2D is a table of inputs and outputs of the combinational logic gate, the visual colour changes of the output "0" (red) and output "1" (blue) can be clearly identified. The mechanisms of analyte induced aggregation or anti-aggregation of Au NPs can be used for the discrimination of different analytes or their combinations under certain conditions. A schematic illustration of this application can be found in Fig. S2 (ESI†).

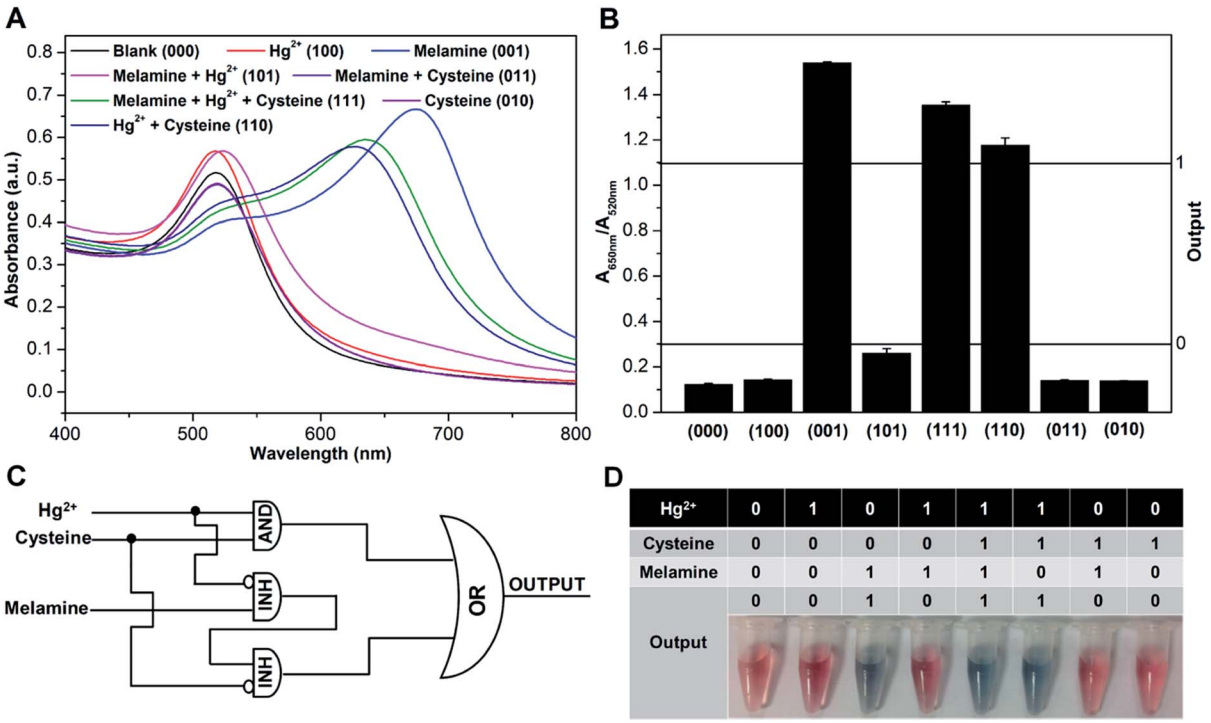

Fig. 2 Combinational logic gate operations (AND, INH, and OR) using colloidal Au NP solution. (A) UV-vis absorption spectra responses of Au NP solutions upon the combinational additions of melamine (6×10^{-5} M), cysteine (3.6×10^{-4} M), and Hg^{2+} (1.8×10^{-4} M). (B) The corresponding signal readouts as a function of $A_{650\ nm}/A_{520\ nm}$. (C) Network map schematically representing the combinations of AND, INH, and OR gates for the logic operations. (D) The inputs and outputs of the colorimetric logic gates. Inset is the corresponding output colour of the colloidal Au NP solutions.

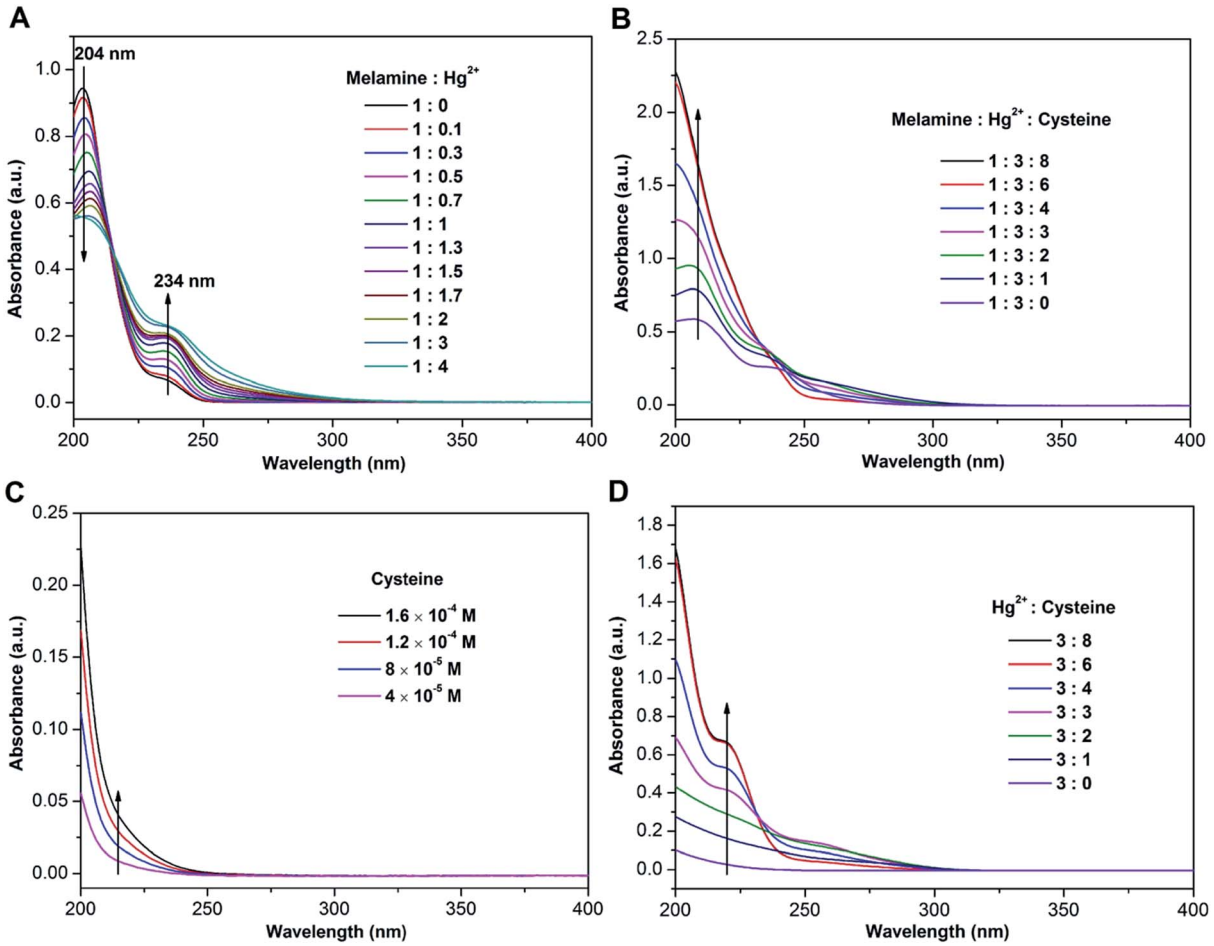

Fig. 3 Interactions between melamine, cysteine, and Hg^{2+} in aqueous solution. UV-vis absorption spectra responses of (A) melamine (2×10^{-5} M) aqueous solution upon the addition of Hg^{2+} at the molar ratio (melamine/Hg^{2+}) ranging from 1 : 0 to 1 : 4, (B) melamine (2×10^{-5} M)–Hg^{2+} (6×10^{-5} M) complex aqueous solution upon the addition of cysteine at the molar ratio (melamine/Hg^{2+}/cysteine) ranging from 1 : 3 : 0 to 1 : 3 : 8, (C) cysteine aqueous solution at the concentration ranging from 4×10^{-5} M to 1.6×10^{-4} M, and (D) Hg^{2+} (6×10^{-5} M) aqueous solution upon the addition of cysteine at the molar ratio (Hg^{2+}/cysteine) ranging from 3 : 0 to 3 : 8.

A competing coordination interaction based mechanism between Hg^{2+}, melamine and cysteine

To better understand the interactions between Hg^{2+}, melamine and cysteine, the coordination reaction between Hg^{2+} and melamine was first investigated through the titration experiments. Fig. 3A shows the absorption spectra changes of the melamine solution on titration with Hg^{2+}. The free melamine in aqueous solution exhibits a strong absorption band at 204 nm and a weak absorption band at 234 nm.[42,44] However, upon the addition of Hg^{2+} to the melamine aqueous solution, the intensity of the absorption band at 234 nm is greatly enhanced, whereas the intensity of the absorption band at 204 nm shows a pronounced decrease, indicating that coordination occurred between Hg^{2+} and melamine. The enhancement of the absorption band at 234 nm and the decrease of the absorption band at 204 nm are both observed by increasing the molar ratio of Hg^{2+} to melamine from 3 : 1 to 4 : 1, implying there is still an excess amount of nitrogen atoms which are not completely coordinated in the solution of Hg^{2+}–melamine complexes at the molar ratio of 3 : 1. A solution of Hg^{2+}–melamine complexes at the molar ratio of 3 : 1 was then chosen to study the ligand replacement reaction of Hg^{2+} upon the addition of cysteine. Fig. 3B shows the evolution of absorption spectra of the Hg^{2+}–melamine complex solution at the molar ratio of 3 : 1 upon the addition of cysteine. The absorption bands in the range of 200 to ~230 nm increase strongly and reach their maxima at the molar ratio of 1 : 3 : 6 (melamine/Hg^{2+}/cysteine). To make sure these increments are not the result of the addition of cysteine itself, the equivalent amounts of cysteine were investigated solely (Fig. 3C). The increments of the band at 200 to ~230 nm induced by the addition of cysteine to the solution of the Hg^{2+}–melamine complex, are about 8 times higher when compared to the increments caused solely by cysteine, suggesting that the Hg^{2+}–melamine complex is transformed into a more stable Hg^{2+}–cysteine complex. We also checked that the absorption spectra changes of the titration of Hg^{2+} solution with cysteine at the same molar ratio ranges from 3 : 0 to 3 : 8. Similar increments of the band at 200 to ~230 nm are observed, indicating that the coordination reaction between Hg^{2+} and cysteine indeed occurs (Fig. 3D). Both of the increments of the bands at

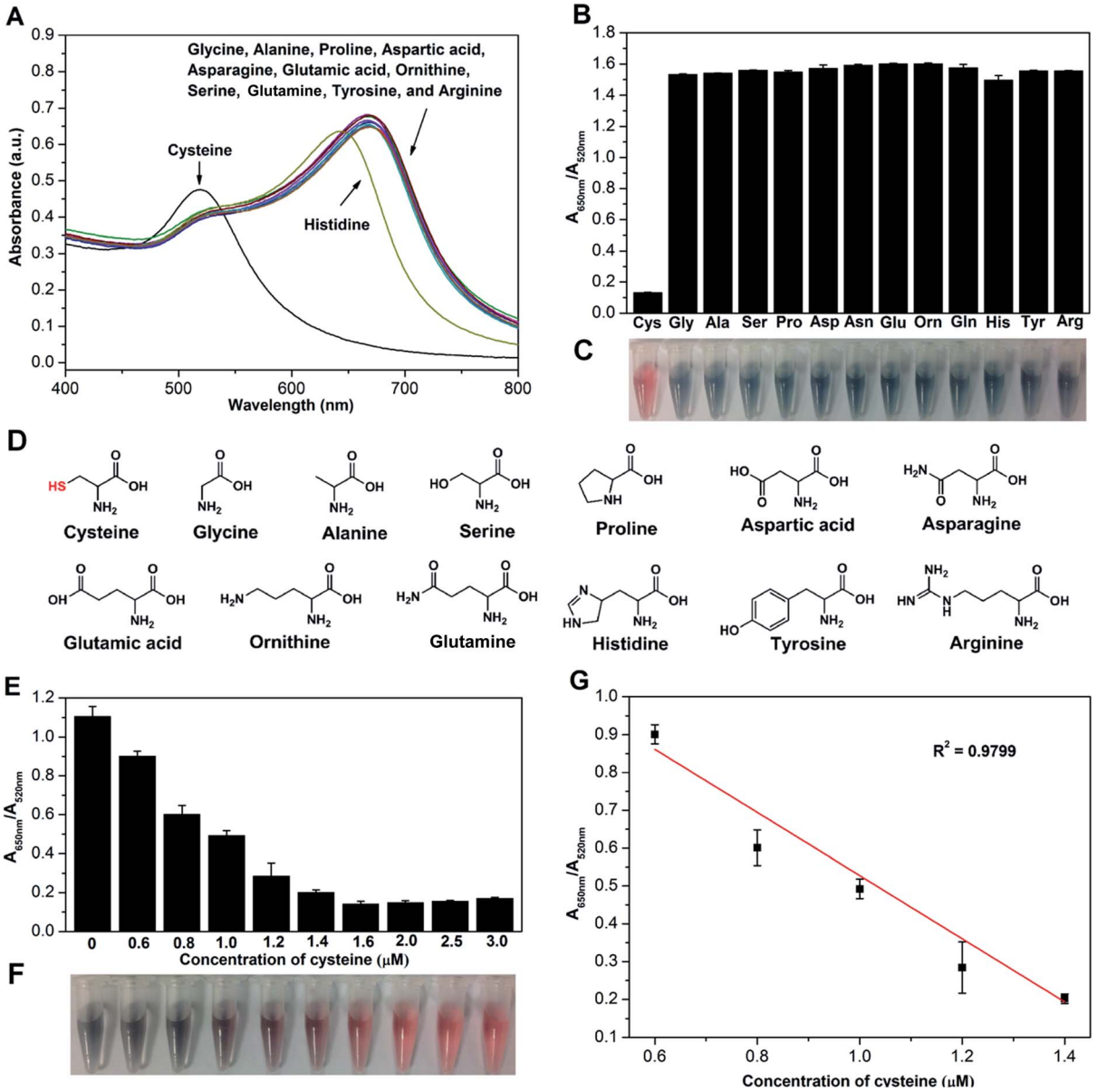

Fig. 4 Visual detection of cysteine. (A) UV-vis absorption spectra responses of Au NP solutions upon the addition of 6×10^{-5} M different amino acids in the presence of 6×10^{-5} M melamine, (B) the corresponding signal readouts in the form of $A_{650\ nm}/A_{520\ nm}$, (C) the colour readouts of the Au NP solutions, and (D) molecular structures of the amino acids. (E) Signal readouts in the form of $A_{650\ nm}/A_{520\ nm}$ of the Au NP solutions upon the addition of cysteine with different concentrations in the presence of 1.4×10^{-6} M melamine, (F) the corresponding visual colour changes of the Au NP solutions, and (G) a linear plot of $A_{650\ nm}/A_{520\ nm}$ as a function of cysteine concentration over the range of 0.6 to 1.4 μM. All the UV-vis absorption spectra and the photos of Au NP solutions were collected after the same time (2 minutes).

200 to ~230 nm reach their maxima when the molar ratio of Hg^{2+} to cysteine is 3 : 6 in the solution of Hg^{2+}–cysteine and Hg^{2+}–melamine–cysteine, implying that a stable complex of Hg^{2+}(cysteine)$_2$ was formed in both systems, with and without melamine, which strongly suggests the complete transition of Hg^{2+}–melamine complexes to Hg^{2+}–cysteine complexes. It is also consistent with many previous reports that cysteine is capable of forming a complex of Hg^{2+}(cysteine)$_2$ with Hg^{2+}, and that the stability constant of the Hg^{2+}(cysteine)$_2$ complex is as high as 2×10^{40}.[45,46] A series of control experiments were also carefully conducted and these results are evident in our proposed mechanisms. These are that cysteine with a sulfhydryl group can protect Au NPs from aggregation in the presence of melamine, and can form more stable complexes with Hg^{2+} through coordination, to destabilize the Au NP colloidal solution in the presence or absence of melamine (Fig. S3 and S4, ESI†).

Detection of melamine, Hg^{2+}, and cysteine in aqueous solution

Au NP colloidal solution was reported to show intrinsic colorimetric sensitivity and selectivity to melamine;[23,41] we also

investigated this in detail (Fig. S5–S7, ESI†). Cysteine has been widely used for inducing the aggregation of Au NPs at high concentration or low pH values for various applications due to the formation of zwitterionic networks involving head-to-head interactions of the deprotonated carboxylate ($-COO^-$) and protonated amine ($-NH_3^+$) groups on adjacent particles.[47] In our work, we found that cysteine could also be employed as a stabilizing agent to prevent the aggregation of Au NPs induced by melamine under certain conditions. Therefore, an unusual application in which the "INH" gate of melamine/cysteine was employed in the selective and sensitive detection of cysteine was devised. Fig. 4A shows the changes in the absorption spectra of Au NPs as a result of the addition of different amino acids in the presence of melamine. It exhibits a high selectivity for cysteine over other amino acids including glycine (Gly), alanine (Ala), serine (Ser), proline (Pro), aspartic acid (Asp), asparagine (Asn), glutamic acid (Glu), ornithine (Orn), glutamine (Gln), histidine (His), tyrosine (Tyr), and arginine (Arg) based on the $A_{650\ nm}/A_{520\ nm}$ values and their corresponding colour readouts (Fig. 4B and C). It can be seen from the molecular structures that only cysteine which is a sulfhydryl-containing amino acid could inhibit the aggregation of Au NPs induced by melamine (Fig. 4D). To evaluate the sensitivity of the assay, the $A_{650\ nm}/A_{520\ nm}$ values of Au NPs were measured after the addition of various concentrations of cysteine in the presence of melamine. As can be seen from Fig. 4E, the intensity ratios of the two absorption bands at 520 and 650 nm gradually decrease with the increasing amount of cysteine. Even when cysteine is at the concentration of 0.6 μM, the decrease of the $A_{650\ nm}/A_{520\ nm}$ value can be still clearly obtained with the UV-vis spectrometer, demonstrating the sensitive response to cysteine. The decrease of the $A_{650\ nm}/A_{520\ nm}$ values results in clear colour changes of Au NP solutions from dark blue to wine red (Fig. 4F). As can be seen from Fig. 4G, in the cysteine concentration range of 0.6 to 1.4 μM, the $A_{650\ nm}/A_{520\ nm}$ value is closely related to the amount of cysteine added to the Au NP solution, which can be used for the quantification of cysteine. Based on a similar strategy, the "INH" gate of melamine/Hg^{2+} can be applied to the selective and sensitive detection of Hg^{2+}. The limit of detection for Hg^{2+} can reach as low as 50 nM (10 ppb) based on the $A_{650\ nm}/A_{520\ nm}$ value (Fig. S8, ESI†).

Conclusion

In summary, a three-input colorimetric logic gate has been designed based on the highly specific coordination and ligand replacement reactions between melamine, cysteine, Hg^{2+}, and Au NPs, and its utility has been established for visual discrimination of melamine, cysteine, and Hg^{2+} in aqueous solution. The "INH" gates of melamine/cysteine and melamine/Hg^{2+} can also be used to quantitate cysteine and Hg^{2+} in solutions on the basis of the measurement of $A_{650\ nm}/A_{520\ nm}$ ratios of Au NPs. The "INH" gate of melamine/cysteine allows the rapid detection of cysteine down to 0.6 μM within 2 minutes. The "INH" gate of melamine/Hg^{2+} provides a rapid detection of Hg^{2+} as low as 50 nM (10 ppb) within 15 minutes. This herein reported concept could be extended to the visual detection of a wide range of organic and biological molecules through properly designing different coordination and ligand replacement reactions based on Au NPs.

Acknowledgements

Q.X. gratefully acknowledges the financial support from Singapore National Research Foundation through its Fellowship grant (NRF-RF2009-06), and Singapore Ministry of Education *via* its two AcRF Tier2 grants (MOE2011-T2-2-051 and MOE2011-T2-2-085). C.C. acknowledges the support from the Central Research Support Funds of Queen's University Belfast *via* a start-up grant. This research is also supported in part by the CAS/SAFEA International Partnership Program for Creative Research Teams.

References

1 http://en.wikipedia.org/wiki/2008_Chinese_milk_scandal.
2 http://www.themalaymailonline.com/world/article/china-seizes-melamine-tainted-yoghurt-candy-in-new-food-scandal#sthash.quKoBjJK.dpuf.
3 P. M. Bolger and B. A. Schwetz, *N. Engl. J. Med.*, 2002, **347**, 1735–1736.
4 R. Janaky, V. Varga, A. Hermann, P. Saransaari and S. S. Oja, *Neurochem. Res.*, 2000, **25**, 1397–1405.
5 M. PukaSundvall, P. Eriksson, M. Nilsson, M. Sandberg and A. Lehmann, *Brain Res.*, 1995, **705**, 65–70.
6 M. T. Goodman, K. McDuffie, B. Hernandez, L. R. Wilkens and J. Selhub, *Cancer*, 2000, **89**, 376–382.
7 J. K. Liu, H. C. Yeo, E. Overvik-Douki, T. Hagen, S. J. Doniger and D. W. Chu, *J. Appl. Physiol.*, 2000, **89**, 21–28.
8 N. Saravanan, D. Senthil and P. Varalakshmi, *Br. J. Urol.*, 1996, **78**, 22–24.
9 W. Droge and E. Holm, *FASEB J.*, 1997, **11**, 1077–1089.
10 I. Perlman, N. Stillman and I. L. Chaikoff, *J. Biol. Chem.*, 1940, **133**, 651–659.
11 W. L. Clevenger, B. W. Smith and J. D. Winefordner, *Crit. Rev. Anal. Chem.*, 1997, **27**, 1–26.
12 R. Kunkel and S. E. Manahan, *Anal. Chem.*, 1973, **45**, 1465–1468.
13 N. H. Bings, A. Bogaerts and J. A. C. Broekaert, *Anal. Chem.*, 2006, **78**, 3917–3945.
14 A. Bernaus, X. Gaona, J. M. Esbri, P. Higueras, G. Falkenberg and M. Valiente, *Environ. Sci. Technol.*, 2006, **40**, 4090–4095.
15 S. Ehling, S. Tefera and I. P. Ho, *Food Addit. Contam.*, 2007, **24**, 1319–1325.
16 G. M. Huang, O. Y. Zheng and R. G. Cooks, *Chem. Commun.*, 2009, 556–558.
17 S. Shahrokhian, *Anal. Chem.*, 2001, **73**, 5972–5978.
18 G. Hignett, S. Threlfell, A. J. Wain, N. S. Lawrence, S. J. Wilkins, J. Davis, R. G. Compton and M. F. Cardosi, *Analyst*, 2001, **126**, 353–357.
19 Y. V. Tcherkas and A. D. Denisenko, *J. Chromatogr. A*, 2001, **913**, 309–313.
20 C. M. Pfeiffer, D. L. Huff and E. W. Gunter, *Clin. Chem.*, 1999, **45**, 290–292.

21 K. L. Ai, Y. L. Liu and L. H. Lu, *J. Am. Chem. Soc.*, 2009, **131**, 9496–9497.
22 F. Chai, C. G. Wang, T. T. Wang, Z. F. Ma and Z. M. Su, *Nanotechnology*, 2010, 21.
23 H. Chi, B. H. Liu, G. J. Guan, Z. P. Zhang and M. Y. Han, *Analyst*, 2010, **135**, 1070–1075.
24 J. J. Du, S. Y. Yin, L. Jiang, B. Ma and X. D. Chen, *Chem. Commun.*, 2013, **49**, 4196–4198.
25 J. S. Lee, P. A. Ulmann, M. S. Han and C. A. Mirkin, *Nano Lett.*, 2008, **8**, 529–533.
26 D. B. Liu, W. S. Qu, W. W. Chen, W. Zhang, Z. Wang and X. Y. Jiang, *Anal. Chem.*, 2010, **82**, 9606–9610.
27 Y. Ma and L. Y. L. Yung, *Anal. Chem.*, 2014, **86**, 2429–2435.
28 K. H. Su, Q. H. Wei, X. Zhang, J. J. Mock, D. R. Smith and S. Schultz, *Nano Lett.*, 2003, **3**, 1087–1090.
29 S. Srivastava, B. L. Frankamp and V. M. Rotello, *Chem. Mater.*, 2005, **17**, 487–490.
30 A. P. de Silva and S. Uchiyama, *Nat. Nanotechnol.*, 2007, **2**, 399–410.
31 Q. S. Mei, C. L. Jiang, G. J. Guan, K. Zhang, B. H. Liu, R. Y. Liu and Z. P. Zhang, *Chem. Commun.*, 2012, **48**, 7468–7470.
32 R. Freeman, T. Finder and I. Willner, *Angew. Chem., Int. Ed.*, 2009, **48**, 7818–7821.
33 K. S. Hettie, J. L. Klockow and T. E. Glass, *J. Am. Chem. Soc.*, 2014, **136**, 4877–4880.
34 X. Q. Liu, R. Aizen, R. Freeman, O. Yehezkeli and I. Willner, *ACS Nano*, 2012, **6**, 3553–3563.
35 M. Zhang and B. C. Ye, *Chem. Commun.*, 2012, **48**, 3647–3649.
36 Z. Z. Huang, H. N. Wang and W. S. Yang, *Nanoscale*, 2014, **6**, 8300–8305.
37 A. Ogawa and M. Maeda, *Chem. Commun.*, 2009, 4666–4668.
38 X. W. Xu, J. Zhang, F. Yang and X. R. Yang, Colorimetric Logic Gates for Small Molecules Using Split/Integrated Aptamers and Unmodified Gold Nanoparticles, *Chem. Commun.*, 2011, **47**, 9435–9437.
39 D. B. Liu, W. W. Chen, K. Sun, K. Deng, W. Zhang, Z. Wang and X. Y. Jiang, *Angew. Chem., Int. Ed.*, 2011, **50**, 4103–4107.
40 A. Ogawa and Y. Susaki, *Org. Biomol. Chem.*, 2013, **11**, 3272–3276.
41 F. Wei, R. Lam, S. Cheng, S. Lu, D. A. Ho and N. Li, *Appl. Phys. Lett.*, 2010, 96.
42 L. L. Li, G. H. Wu, T. Hong, Z. Y. Yin and D. Sun, *ACS Appl. Mater. Interfaces*, 2014, **6**, 2865–2871.
43 S. S. R. Dasary, A. K. Singh, D. Senapati, H. T. Yu and P. C. Ray, *J. Am. Chem. Soc.*, 2009, **131**, 13806–13812.
44 M. J. S. Dewar and L. Paolo, *Trans. Faraday Soc.*, 1957, **53**, 261–271.
45 B. V. Cheesman, A. P. Arnold and D. L. Rabenstein, *J. Am. Chem. Soc.*, 1988, **110**, 6359–6364.
46 W. E. Van Der Linden and C. Beers, *Anal. Chim. Acta*, 1973, **68**, 143–154.
47 A. Mocanu, I. Cernica, G. Tomoaia, L. D. Bobos and O. Horovitz, *Colloids Surf., A*, 2009, **338**, 93–101.